

A STOCHASTIC APPROACH TO COMPUTE NOISE GENERATION  
AND RADIATION OF FREE TURBULENT FLOWS

C. Bailly

Ph. D.

E.M2.C. Laboratory, Ecole Centrale Paris  
Grande Voie des Vignes, 92295 Châtenay-Malabry, France

P. Lafon

Research Engineer, Member AIAA.

Département Acoustique et Mécanique Vibratoire, EDF  
1 Av. du Gal de Gaulle, 92141 Clamart, France

S. Candel

Professor, Member AIAA.

E.M2.C, Ecole Centrale Paris  
Grande Voie des Vignes, 92295 Châtenay-Malabry, France

Abstract

This paper deals with a Stochastic Noise Generation and Radiation (SNGR) model to compute turbulent mixing noise. Two problems must be solved in the framework of an acoustic analogy. First, a wave operator must be derived for sound waves travelling in any mean flow. An expression of the source term is then deduced by using the conservation laws of motion, and can be simplified with classic assumptions of aeroacoustics in the case of subsonic mixing noise. Secondly, the knowledge of the turbulence velocity field is required to compute this source term. Finally, the radiated acoustic field is calculated numerically by solving the inhomogeneous acoustic wave equation. In this study, the wave operator is the system of the linearized Euler's equations and the space-time turbulence velocity field is generated by a sum of random Fourier modes. This method is applied to the case of a cold round subsonic jet at  $M = 0.86$  and results are compared with available experimental data.

1. INTRODUCTION: PROPAGATION IN NON-UNIFORM MEAN FLOW

The simplest wave equation that one can exactly derive from the fundamental conservation laws of motion is Lighthill's equation:<sup>20,21</sup>

$$\frac{\partial^2 \rho}{\partial t^2} - c_0^2 \frac{\partial^2 \rho}{\partial x_i \partial x_i} = \frac{\partial^2 T_{ij}}{\partial x_i \partial x_j} \quad (1)$$

where  $\rho$ ,  $p$ ,  $u$ ,  $\tau$  and  $T$  are respectively the density, the pressure, the velocity, the viscous stress tensor and Lighthill's tensor  $T_{ij} = \rho u_i u_j + (p - c_0^2 \rho) \delta_{ij} - \tau_{ij}$ . Here we assume the medium external to the flow is homogeneous and at rest,  $c_0$  being the constant speed in this ambient medium. The free-space Green function of this wave operator is known what explains the success of Lighthill's analogy in many various studies.<sup>1-3,6,11-14,26,29</sup> However mean flow effects on the acoustic waves propagation are not taken into account and they are known yet to modify the aerodynamic noise spectrum and directivity. Phillips<sup>27</sup> replaced Lighthill's equation by a convected wave equation where a part of the mean flow effects were included in the wave operator rather than in the source term. Introducing the more useful variable  $\pi = \ln p$  logarithm of the pressure, Phillips' equation reads:

$$\frac{d^2 \pi}{dt^2} - \frac{\partial}{\partial x_i} \left( c_0^2 \frac{\partial \pi}{\partial x_i} \right) = \gamma \frac{\partial u_i}{\partial x_j} \frac{\partial u_j}{\partial x_i} + \frac{d}{dt} \left( \frac{1}{c_0} \frac{ds}{dt} \right) - \frac{\partial}{\partial x_i} \left( \frac{\gamma}{\rho} \frac{\partial \pi_{ij}}{\partial x_j} \right) \quad (2)$$

where  $\gamma = c_p/c_v$  is the specific heats ratio. One sees that the main source term for jet noise contains only components of the velocity field unlike Lighthill's source term. The free-space Green function is known in the case of a plug flow.<sup>25</sup> For high Reynolds number, the viscous stress tensor can be neglected. Furthermore, one assumes viscous dissipation and heat conduction effects are negligible in sound generation and propagation. Then in assuming a parallel sheared mean flow:  $u_i = U(x_2) \delta_{1i} + u'_i$ , Phillips' equation (3) may be written in the form:

$$\frac{D^2 \pi'}{Dt^2} - \frac{\partial}{\partial x_i} \left( c_0^2 \frac{\partial \pi'}{\partial x_i} \right) = 2\gamma \frac{\partial u'_2}{\partial x_1} \frac{dU}{dx_2} + \gamma \left\{ \frac{\partial u'_i}{\partial x_j} \frac{\partial u'_j}{\partial x_i} - \frac{\partial u'_i}{\partial x_j} \frac{\partial u'_j}{\partial x_i} \right\} \quad (3)$$

where

$$\frac{D}{Dt} = \frac{\partial}{\partial t} + U \frac{\partial}{\partial x_1}$$

is the convective time derivation operator. Besides, one knows that linearized Euler's equations govern acoustic wave propagation. So, the associated wave equation should be identical to the previous homogeneous equation. But it is not the case.<sup>9,22</sup> Indeed, assuming a global isentropic relation  $dp = c_0^2 d\rho$ , the wave equation derived from the linearized Euler's equation is given by:

$$\frac{D^2 \pi'}{Dt^2} - \frac{\partial}{\partial x_i} \left( c_0^2 \frac{\partial \pi'}{\partial x_i} \right) - 2\gamma \frac{dU}{dx_2} \frac{\partial u'_2}{\partial x_1} = 0 \quad (4)$$

In order to eliminate the term containing velocity fluctuations of the wave operator, we must again apply the  $D/Dt$  operator to the last equation. One finally obtains:

$$\frac{D}{Dt} \left\{ \frac{D^2 \pi'}{Dt^2} - \frac{\partial}{\partial x_i} \left( c_0^2 \frac{\partial \pi'}{\partial x_i} \right) \right\} + 2 \frac{dU}{dx_2} \frac{\partial}{\partial x_1} \left( c_0^2 \frac{\partial \pi'}{\partial x_2} \right) = 0 \quad (5)$$

This equation shows that Phillips' wave operator does not contain all the terms that appear in (5). On the other hand, in the case of a sheared mean flow, the simplest wave equation for the acoustic variable  $\pi'$  is a third order differential equation. Lilley<sup>22</sup> derived a third order wave equation from Phillips'

equation with this idea. Thus, in applying the  $D/Dt$  operator to Phillips' equation (3), it follows:

$$\begin{aligned} \frac{d}{dt} \left\{ \frac{d^2 \pi}{dt^2} - \frac{\partial}{\partial x_i} \left( c^2 \frac{\partial \pi}{\partial x_i} \right) \right\} + 2 \frac{\partial u_i}{\partial x_j} \frac{\partial}{\partial x_i} \left( c^2 \frac{\partial \pi}{\partial x_j} \right) \\ = -2\gamma \frac{\partial u_i}{\partial x_j} \frac{\partial u_j}{\partial x_k} \frac{\partial u_k}{\partial x_i} + \text{other terms} \end{aligned} \quad (6)$$

where the viscous contribution and the entropy fluctuations are neglected. The free-space Green function of the Lilley's equation is unknown and it is difficult to solve numerically a third order wave equation, unlike the linearized Euler's equations. Moreover, in the case of a nonuniform mean flow, acoustic and hydrodynamic fluctuations can not be clearly separated by a wave operator.<sup>7,15,24,31</sup> So, computation of the acoustic field by solving linearized Euler's equations seems an interesting way. An analysis of the acoustic analogy associated with linearized Euler's equations has been developed.<sup>2,5</sup> The following system of two first-order equations has been retained:

$$\begin{cases} \frac{\partial p'}{\partial t} + u_{j0} \frac{\partial p'}{\partial x_j} + u'_j \frac{\partial p_o}{\partial x_j} + \gamma p_o \frac{\partial u'_j}{\partial x_j} + \gamma p' \frac{\partial u_{j0}}{\partial x_j} = 0 \\ \frac{\partial u'_i}{\partial t} + u_{j0} \frac{\partial u'_i}{\partial x_j} + u'_j \frac{\partial u_{i0}}{\partial x_j} + \frac{1}{\rho_o} \frac{\partial p'}{\partial x_i} - \frac{p'}{\rho_o^2 c_o^2} \frac{\partial p_o}{\partial x_i} = S_i \end{cases} \quad (7)$$

where the source term reads as follows:

$$S_i = - \left\{ u_{jt} \frac{\partial u_{it}}{\partial x_j} - u_{jt} \frac{\partial u_{it}}{\partial x_j} \right\}$$

The subscript  $o$  designates a value of the mean flowfield and the subscript  $t$  a value of the turbulent field.  $u'$  and  $p'$  are the acoustic velocity and pressure. The left hand side of (7) is the system of the linearized Euler's equations around a stationary mean flow ( $U_o, p_o, \rho_o$ ). The right hand side of this system is the acoustic source term, which is nonlinear in fluctuating part of the velocity. However its time average is zero. The previous system (7) is obtained with the three following assumptions. Acoustic pressure fluctuations are isentropic, the turbulent velocity is incompressible, and only the first order interaction between the mean flow and the acoustic field is retained. In other words, phenomena such as scattering of sound by turbulence are assumed to be negligible.

Finally, to compute the sound field, one carries out the three following steps:

- (i) An aerodynamic calculation of the mean flow is performed by solving the averaged Navier-Stokes equations with a  $k - \epsilon$  turbulence closure.
- (ii) A space-time stochastic turbulent velocity field is generated as a sum of random Fourier modes.
- (iii) The propagation system (7) is solved. In the left hand side, one uses values of the mean flowfield calculated in the first step as coefficients of the two first-order differential equations, and on the other hand, the acoustic source term  $S$  is calculated from the synthesized turbulent field.

Section 2 shows how one may synthesize a space-time turbulent velocity field with suitable statistical properties. The three steps are then carried out in section 3 in the case of a high-subsonic jet.

## 2. A SPACE-TIME STOCHASTIC TURBULENT VELOCITY FIELD

A method to simulate a spatial stochastic turbulent velocity field has been developed by Kraichnan<sup>18</sup> and Karweit.<sup>16</sup> One uses here this Fourier mode approach but a time evolution of the turbulent field  $u$  is introduced by writing that:

$$\frac{\partial u}{\partial t} + U_c \cdot \nabla u = 0$$

where  $U_c$  is the convection velocity. In all this section, the subscript  $t$  which designates the turbulent velocity field is omitted. Thus, the turbulent velocity field is given by the following sum of  $N$  modes:

$$u(x, t) = 2 \sum_{n=1}^N \tilde{u}_n \cos [k_n \cdot (x - tU_c) + \psi_n + \omega_n t] \sigma_n \quad (8)$$

where  $k_n$  is the wave vector picked randomly on a sphere to ensure a statistical isotropy at time zero. As a consequence of the incompressibility of the turbulent velocity field,  $k_n \cdot \sigma_n = 0$  for each mode  $n$ .  $\psi_n$  is chosen with uniform probability to obtain an homogeneous field, and  $\omega_n$  is picked with gaussian probability such as:

$$p(\omega) = \frac{1}{\omega_t \sqrt{2\pi}} \exp \left( -\frac{\omega^2}{2\omega_t^2} \right) \quad \text{with} \quad \omega_t = 2\pi \frac{\epsilon}{k}$$

where  $k$  is the kinetic energy per mass unit and  $\epsilon$  the rate of dissipation, that is to say the rate of transfert of kinetic energy per mass unit and per time unit. These two local values of the turbulent field allow to estimate the integral length scale  $L$ :

$$L = \int_0^\infty f(\tau) d\tau \simeq \frac{k^{3/2}}{\epsilon}$$

and a characteristic angular frequency  $\omega_t \simeq 2\pi\epsilon/k$ . These two scales must be associated to the more energizing structures of turbulence. Besides, the Karman-Howarth longitudinal correlation function  $f(\tau) = u_1(0, 0, 0) u_1(\tau, 0, 0)$  is related to the energy spectrum  $E(k)$  for an isotropic turbulence by the following general expression:

$$f(\tau) = \frac{2}{\bar{u}^2} \int_0^\infty \left( \frac{\sin(kr)}{k^3 r^3} - \frac{\cos(kr)}{k^2 r^2} \right) E(k) dk \quad (9)$$

with  $\bar{u}^2 = 2/3k$ . The amplitude  $\tilde{u}$  of each mode is determined from a modified Von Karman spectrum to simulate the complete spectral range:

$$\begin{cases} \tilde{u}_n = \sqrt{E(k_n) \Delta k_n} \\ E(k) = \alpha \frac{\bar{u}^2}{k_\epsilon} \frac{(k/k_\epsilon)^4}{[1 + (k/k_\epsilon)^2]^{17/6}} \exp \left[ -2 \left( \frac{k}{k_n} \right)^2 \right] \end{cases}$$

where  $k_n = \epsilon^{1/4} \nu^{3/4}$  is the Kolmogorov wave number. The parameters  $\alpha$  and  $k_\epsilon$  of the spectrum are determined from the two integral relations which define  $k$  and  $\epsilon$ :

$$k = \int_0^\infty E(k, t) dk$$

$$\epsilon = 2\nu \int_0^\infty k^2 E(k, t) dk$$

A realization of the spatial distribution of the simulated turbulent field at  $t = 0$  with  $N = 200$  modes is plotted in figure 1. The size of the square domain is  $4L$ . Figure 2 displays

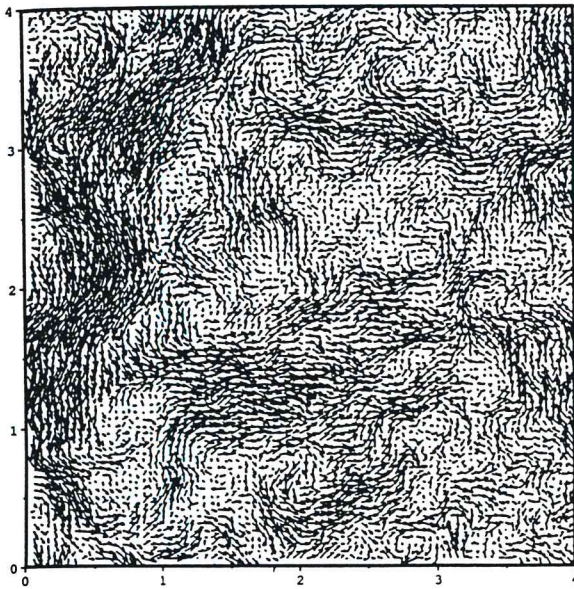


Figure 1: Spatial distribution of the simulated turbulent velocity field at  $t = 0$  with  $N = 200$  modes,  $k = 900 \text{ m}^2 \cdot \text{s}^{-2}$  and  $\epsilon = 1.5 \times 10^6 \text{ m}^2 \cdot \text{s}^{-3}$ . The size of the square domain is  $4L$ , where  $L$  is the integral length scale.

the simulated correlation function  $f$  and the exact expression (9). At time zero, the turbulent field is isotropic. As a consequence, the Reynolds tensor  $\overline{u_i u_j}$  is diagonal and the following statistical moments verify:

$$\left\{ \begin{array}{l} \overline{u_i} = 0 \\ \overline{u_i u_j} = \frac{2}{3} k \delta_{ij} \\ S_i = \frac{\overline{u_i^3}}{(\overline{u_i^2})^{3/2}} = 0 \text{ for the skewness factor,} \\ T_i = \frac{\overline{u_i^4}}{(\overline{u_i^2})^2} = 3 \text{ for the Kurtosis factor.} \end{array} \right.$$

However, since the turbulent field is convected by the mean flow, it is not frozen and the peak of the cross correlation function  $f$  decreases with the time  $\tau$  of separation. One can show<sup>2</sup> that the correlation function can be expressed as follows:

$$R_{ii}(\mathbf{r}, \tau) = \exp\left(-\frac{\tau^2 \omega_i^2}{2}\right) R_{ii}(\mathbf{r} - \tau \mathbf{U}_c, 0)$$

where  $R_{ii}(\mathbf{r}, \tau) = \overline{u_i(0,0) u_i(\mathbf{r}, \tau)}$ . The simulated longitudinal correlation function  $f(\mathbf{r}, \tau) = R_{11}(\mathbf{r}, \tau) / \overline{u^2}$ , where  $\mathbf{r}$  is the distance and  $\tau$  the time of separation, is plotted in figure 3. The statistical average is performed over 64 space-time realizations. With this modeling, the turbulent velocity field exhibits a convective feature.

### 3. APPLICATION TO THE CASE OF A HIGH-SUBSONIC JET

The model is now applied to the case of a free subsonic jet at  $M = 0.86$ . The geometry is based on the experimental configuration of Lush<sup>23</sup> and results are compared to available experimental data.<sup>23,30</sup>

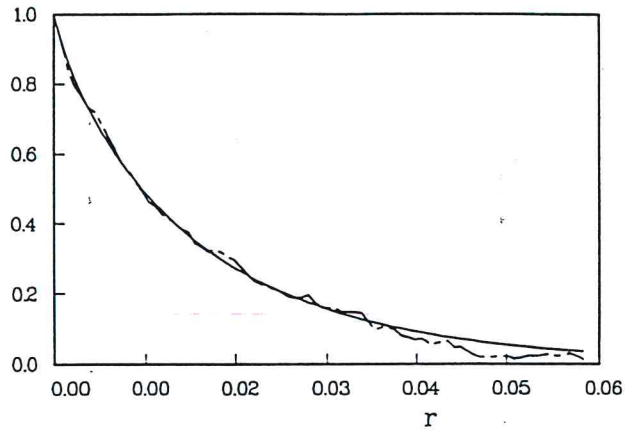


Figure 2: — Simulated longitudinal correlation function  $f(\mathbf{r}) = R_{11}(\mathbf{r}, 0, 0) / \overline{u^2}$  — and - - - analytical expression.

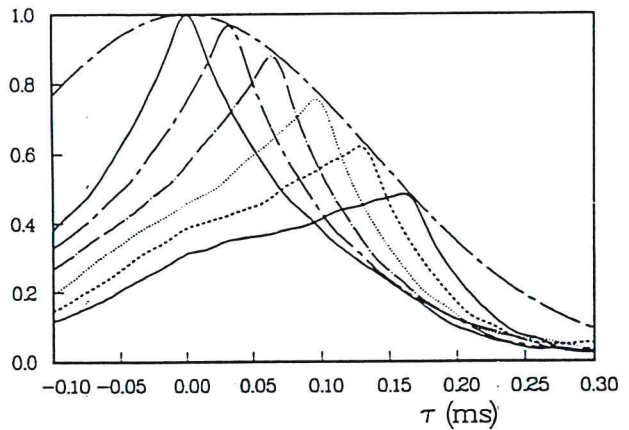


Figure 3: Simulated longitudinal correlation function  $f(\mathbf{r}, \tau)$ . The statistical average is performed over 64 space-time realizations where  $\mathbf{r}$  is the distance and  $\tau$  is the time of separation. —  $f(0, \tau)$ , - - -  $f(r_1, \tau)$ , - · -  $f(r_2, \tau)$ , · · ·  $f(r_3, \tau)$ , - - -  $f(r_4, \tau)$ , - - -  $f(r_5, \tau)$ .

#### 3.1 Aerodynamic results

In a first step, the mean flowfield is calculated as a numerical solution of the average Navier-Stokes equations associated with a  $k - \epsilon$  turbulent closure. These calculations are carried out with an axisymmetric compressible version of the ESTET code developed by the "Laboratoire National Hydraulique" of the "Direction des Etudes et Recherches d'Electricite de France". The computation domain has  $20D$  in the axial direction, with a diameter nozzle  $D$  of  $0.025 \text{ m}$ . Comparisons of the mean axial velocity, the self-similar radial profiles of the mean axial velocity and the turbulence intensity have been done<sup>2,3</sup> with experimental measurements.

#### 3.2 Acoustic results

The calculation of acoustic propagation is performed on a mesh of  $551 \times 701$  points with a spatial step of  $\Delta x = 1.5 \times 10^{-3} \text{ m}$  to simulate a large range of turbulence wave numbers. Also the time step is  $\Delta t = 2.8 \times 10^{-6} \text{ s}$  corresponding to a Strouhal number of  $S_t = 2.8$  for Lush's configuration. This computational domain allows to record the time pressure field on a circle of radius  $R = 33D$  centered on the nozzle exit plane (see figure 4). A sponge zone allows to eliminate all the

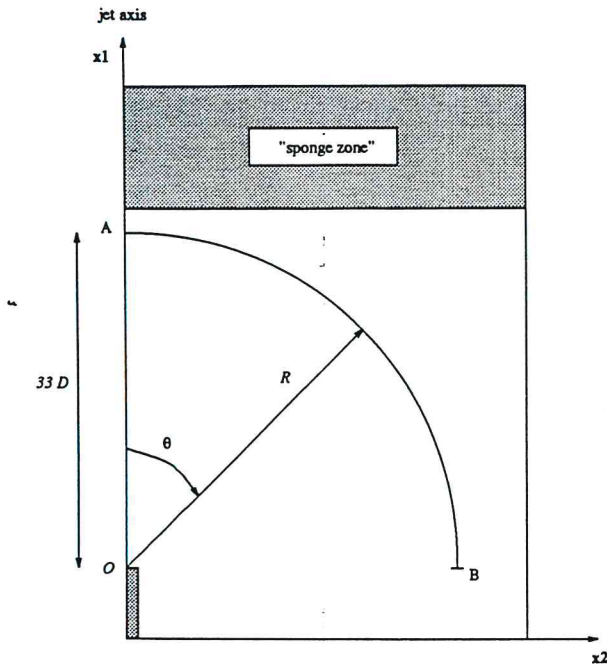


Figure 4: Sketch of the acoustic computational domain.

waves (acoustic waves & instability waves) without feedback in the physical domain (non-reflecting boundary conditions). The propagation equations (7) are solved with the axisymmetric version of the EOLE code developed by the "Direction des Etudes et Recherches d'Electricité De France". The method used in EOLE is based on a fractional step scheme and relies on solutions of one-dimensional problems in terms of a weak formulation.<sup>10</sup> Numerical tests indicate that sound wave propagation is calculated with little dispersion and dissipation. Some applications to the propagation in hot jets show that the effects of convection and refraction are retrieved in the predicted sound field.<sup>19</sup> The CPU time per iteration and per node is of order of  $1.8 \times 10^{-5}$ s on a Cray C98.

Computation of axisymmetric propagation implies that the acoustic sources are completely correlated in the azimuthal direction. Indeed each source point represents an annular set of points which are subjected to the same turbulent fluctuations. So, a directivity factor is introduced and an overestimation of the intensity level is expected.

To perform the acoustic propagation, in a first step the mean flow field is projected on the acoustic mesh, where the propagation calculation will be carried out. Then, the turbulent domain which contributes to the radiated acoustic field is identified as the set of points where the mean velocity gradient and so the kinetic energy are highest.<sup>2,3,6</sup> On this source domain, the stochastic turbulent velocity field is generated with the method described in section 2, and the source term  $S$  is calculated. The two first order differential equations of the system (7) are then solved.

Figure 5 shows the positive pressure contours of the last time step. One observes instability waves near the jet axis travelling at mean flow speed. Acoustic sources are close to the jet axis from  $5D$  to  $10D$  downstream the nozzle, as showed by the wave fronts. The acoustic pressure signal recorded for  $\theta = 90^\circ$  is plotted in figure 6. At time zero, the initial acoustic field is taken as zero in all the computational domain. There is also a time delay corresponding in a first approximation to  $R/c_0$ . The same signal is recorded for  $\theta = 0^\circ$  and is dis-

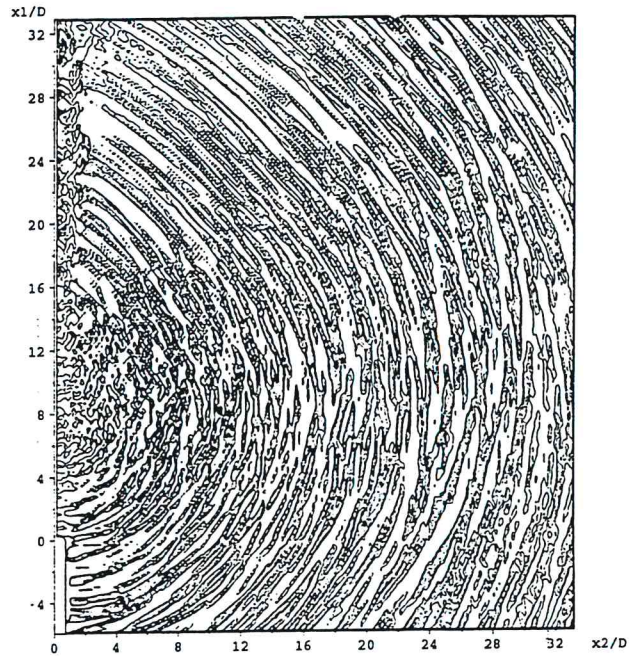


Figure 5: Positive pressure contours at the last time step. One observes the presence of instability waves near the jet axis. The acoustic sources are located from  $5D$  to  $10D$  downstream the nozzle.

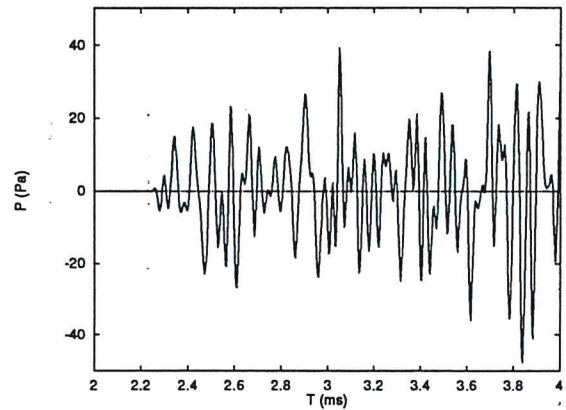


Figure 6: Pressure signal recorded for  $\theta = 90^\circ$ ,  $R = 33D$ .

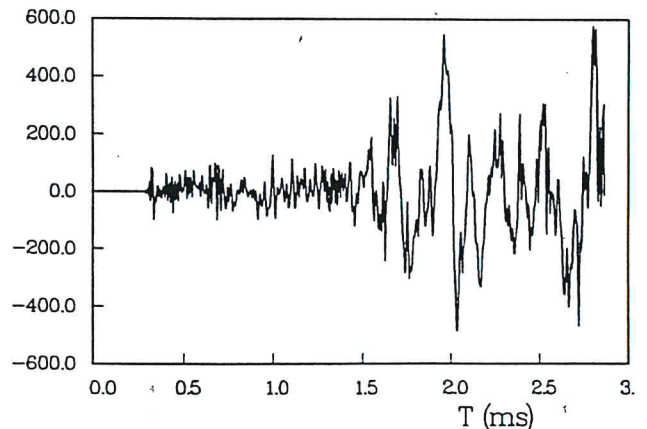


Figure 7: Pressure signal recorded for  $\theta = 0^\circ$ ,  $R = 33D$ .

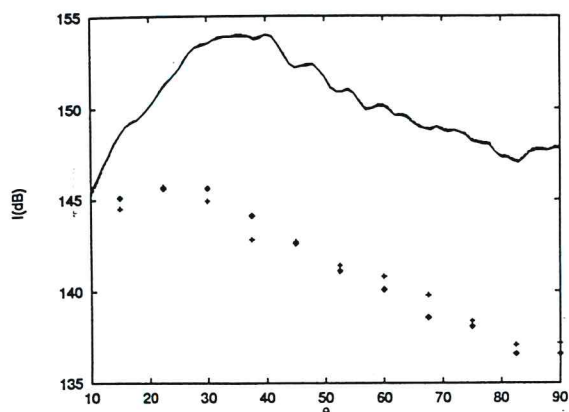


Figure 8: Acoustic directivity in dB (ref.  $10^{-12}$  W.m<sup>-2</sup>). Calculated —. Measured:  $\circ$  Lush<sup>23</sup>  $\triangle$  Tanna.<sup>30</sup>

played in figure 7. In this case, the point is located on the jet axis and after a time delay, one observes in a first time an acoustic wave travelling at the speed  $U + c$ . Then, one records instability waves travelling only at the speed  $U$  with a higher amplitude. In fact, instability waves are generated by interaction between the acoustic field and the nonuniform mean flow. In the uniform mean flow case, it is possible to show that the interaction between the acoustic field and the mean flow does not produce non-acoustic pressure perturbations. In other words, acoustic fluctuations can be separated from the hydrodynamic fluctuations by a wave operator.

The acoustic intensity is plotted in figure 8. Refraction and convection effects are observed on the acoustic intensity. However the acoustic level is overestimated, and do not decreases correctly when  $\theta$  increases.

## CONCLUSION

The original feature of the present contribution is to combine a stochastic turbulent field with modern computational fluid dynamics methods to calculate the acoustic field. With this approach, one takes into account the mean flow effects on the acoustic waves propagation. Comparisons with available measurements are very encouraging. However, some difficulties remain concerning the axisymmetric calculation of the propagation. Other tests are at present performed to validate the stochastic turbulent velocity field, and more generally the SNGR model.

## Reference

- [1] BAILLY, C., BÉCHARA, W., LAFON, P. & CANDEL, S. 1993 Jet noise predictions using a  $k - \epsilon$  turbulence model, *15th Aeroacoustics Conference, AIAA Paper 93-4412*, October 25-27, Long Beach, C.A.
- [2] BAILLY, C. 1994 Modélisation du rayonnement acoustique des écoulements turbulents libres subsoniques et supersoniques, Ph.D. thesis, Ecole Centrale Paris, 1994-19.
- [3] BAILLY, C., LAFON, P. & CANDEL, S. 1994 Computation of subsonic and supersonic jet mixing noise using a modified  $k - \epsilon$  turbulence model for compressible free shear flows, *Acta Acustica*, **2**(2), 101-112.
- [4] BAILLY, C., LAFON, P. & CANDEL, S. 1994 Stochastic approach to noise modelling for free turbulent flows, *Flow acoustics: a technology audit*, Ecole Centrale de Lyon, France, 11-13 July.
- [5] BÉCHARA, W., *et al.* 1994 Stochastic approach to noise modeling for free turbulent flows, *AIAA Journal*, **32**(3), 455-463.
- [6] BÉCHARA, W., LAFON, P., BAILLY, C. & CANDEL, S. 1995 Application of a  $k - \epsilon$  model to the prediction of noise for simple and coaxial free jets, *J. Acoust. Soc. Am.*, **97**(5), 1-14.
- [7] CHU, B.T. & KOVASZNYI, L.G.S. 1958 Non-linear interactions in a viscous heat-conducting compressible gas, *J. Fluid Mech.*, **3**(5), 494-514.
- [8] CRIGHTON, D. 1975 Basic principles of aerodynamic noise generation, *Prog. Aerospace Science* **16**(1), 31-96.
- [9] DOAK, P.E. 1972 Analysis of internally generated sound in continuous materials: 2. A critical review of the conceptual adequacy and physical scope of existing theories of aerodynamic noise, with special reference to supersonic jet noise, *J. Sound Vib.*, **25**(2), 263-335.
- [10] ESPOSITO, P. 1987 A new numerical method for wave propagation in a complex flow, *5th International Conference on Numerical Methods in Laminar and Turbulent Flow*, Montréal, July.
- [11] FLOWERS, WILLIAMS, J.E. 1963 The noise from turbulence convected at high speed, *Philosophical Transactions of Royal Society of London A* **255**, 469-503.
- [12] GOLDSTEIN, M.E. & ROSENBAUM, B. 1973 Effect of anisotropic turbulence on aerodynamic noise, *J. Acoust. Soc. Am.*, **54**(3), 630-645.
- [13] GOLDSTEIN, M.E. & HOWES, W.L. 1973 New aspects of subsonic aerodynamic noise theory, *NASA technical Note*, D-7158.
- [14] GOLDSTEIN, M.E. 1976 *Aeroacoustics*, McGraw-Hill, New York.
- [15] HOWE, M.S. 1975 Contributions to the theory of aerodynamic sound, with application to excess jet noise and the theory of the flute, *J. Fluid Mech.*, **71**(4), 625-673.
- [16] KARWEIT, M., BLANC-BENON, P. JUVÉ D., & COMTE-BELLOT, G. 1991 Simulation of the propagation of an acoustic wave through a turbulent velocity field: A study of phase variance, *J. Acoust. Soc. Am.*, **89**(1), 52-62.
- [17] KISTLER, A.L. & CHEN, W.S. 1962 The fluctuating pressure field in a supersonic turbulent boundary layer, *J. Fluid Mech.*, **16**(1), 41-64.
- [18] KRAICHNAN, R.H. 1970 Diffusion by a random velocity field, *Phys. Fluids*, **13**(1), 22-31.
- [19] LAFON, P. 1989 Propagation acoustique bidimensionnelle. Deux applications du code EOLE, *Direction des Etudes et Recherches d'Electricité de France*, HP 54/89.010.
- [20] Lighthill, M.J. 1952 On sound generated aerodynamically - I. General theory, *Proceedings of the Royal Society of London*, **A211**, 1107, 564-587.

- [21] LIGHTHILL, M.J. 1954 On sound generated aerodynamically - II. Turbulence as a source of sound, *Proceedings of the Royal Society of London*, A222, 1148, 1-32.
- [22] LILLEY, G.M. 1972 The generation and radiation of supersonic jet noise. Vol. IV - Theory of turbulence generated jet noise, noise radiation from upstream sources, and combustion noise. Part II: Generation of sound in a mixing region, *Air Force Aero Propulsion Laboratory*, AFAPL-TR-72-53.
- [23] LUSH, P.A. 1971 Measurements of subsonic jet noise and comparison with theory, *J. Fluid Mech.*, 46(3), 477-500.
- [24] MAESTRELLO, L., BAYLISS, A. & TURKEL, E. 1981 On the interaction of a sound pulse with the shear layer of an axisymmetric jet, *J. Sound Vib.*, 74(2), 281-301.
- [25] MANI, R. 1976 The influence of jet flow on jet noise. Part I. The noise of unheated jets, *J. Fluid Mech.*, 73(4), 753-778.
- [26] PAO, S.P. & LOWSON, M.V. 1970 Some applications of jet noise theory, *8th Aerospace Sciences Meeting, New York*, AIAA Paper 70-223.
- [27] PHILLIPS, O.M. 1960 On the generation of sound by supersonic turbulent shear layers, *J. of Fluid Mech.* 9(1), 1-28.
- [28] RIBNER, H.S. 1964 The generation of sound by turbulent jets, *Advances in Applied Mechanics*, Academic Press, New York, Vol. VIII, 103-182.
- [29] RIBNER, H.S. 1969 Quadrupole correlations governing the pattern of jet noise, *J. of Fluid Mech.*, 38(1), 1-24.
- [30] TANNA, H.K., DEAN, P.D. & BURRIN, R.H. 1976 The generation and radiation of supersonic jet noise, Vol. III Turbulent mixing noise data, *Air Force Aero Propulsion Laboratory*, AFAPL-TR-76-65.
- [31] YATES, J.E. 1978 Application of the Bernoulli enthalpy concept to the study of vortex noise and jet impingement noise, NASA, 2987.